A Monte Carlo method for small signal analysis of the Boltzmann equation

H. Kosina,[a] M. Nedjalkov, and S. Selberherr
Institute for Microelectronics, TU-Vienna, Gusshausstrasse 27–29, A-1040 Vienna, Austria

(Received 27 October 1999; accepted for publication 31 January 2000)

An approach for analysis of the small signal response of carriers in semiconductors is presented. The response to an electric field impulse is explained in terms of a relaxation process governed by a Boltzmann equation. New Monte Carlo algorithms for the direct simulation of the impulse response are presented and existing algorithms are discussed in a unified way. © *2000 American Institute of Physics.* [S0021-8979(00)06109-0]

I. INTRODUCTION

Knowledge of the small signal response of the carrier system is important to forecast the performance of modern semiconductor devices. A differential response function gives the relationship between a small harmonic perturbation $\mathbf{E}_1 e^{i\omega t}$, which is superimposed on a stationary field $\mathbf{E}_s$, and the induced changes in the mean $\langle A\rangle$ of a physical quantity $A(\mathbf{k})$. The complex amplitude $\langle A\rangle_1$ of the oscillation atop the stationary value $\langle A\rangle_s$ is linear in $\mathbf{E}_1$, $\langle A\rangle_1(\omega) = K_A(\omega)\mathbf{E}_1$. Accordingly, the differential response function K_A is the gradient of the response $\langle A\rangle_1$ with respect to $\mathbf{E}_1$. Of particular interest is the tensor of the differential mobility $K_{\mathbf{v}} = \mu(\omega)$ of the velocity response: $\langle \mathbf{v}\rangle_1(\omega) = \mu(\omega)\mathbf{E}_1$.

Linked by the Fourier transform, analyses in the time and the frequency domains provide equivalent information. Furthermore, the response $\langle A\rangle_1(t)$ to a perturbation $\mathbf{E}_1(t)$ of a general time dependence can be calculated from knowledge of the impulse response $\langle A\rangle_{\mathrm{im}}(t)$. Thus finding the response of the carrier system to an electric field impulse is the main task of small signal analysis.

Monte Carlo simulations have been utilized for more than 2 decades[1] to explore the small signal response. Various algorithms have been proposed in the literature, which assume either a stationary or a transient electric field. In this work an approach is presented, which allows us to develop novel Monte Carlo algorithms, and which also assists in understanding some of the existing algorithms. The impulse response is interpreted as the result of a relaxation process.

The basic concepts of existing Monte Carlo algorithms are summarized in Sec. II. In Sec. III a new approach is introduced in the framework of the Boltzmann equation (BE) linearized with respect to the field. The related Monte Carlo algorithms are described in Sec. IV. In Sec. V simulation results for Si and GaAs are presented and discussed. Some peculiarities of the response of carriers in GaAs at low temperatures are explained in terms of the developed model.

[a]Author to whom correspondence should be addressed; electronic mail: kosina@iue.tuwien.ac.at

II. EXISTING MONTE CARLO ALGORITHMS

A. Stationary field description

The steady-state algorithms are based on the theory of correlation functions.[2] The linear response to an impulse in the electric field is directly simulated. The particle trajectories evolve under the action of a stationary electric field. Due to linearity the calculated response functions are independent of the amplitude of the impulse.

A single-particle algorithm is proposed in Ref. 3. The field vectors $\mathbf{E}_1$ and $\mathbf{E}_s$ are assumed to be collinear. A response function is represented by the difference of the before and after scattering averages:

$$\langle A\rangle_i(t) = K_A(t)E_1 = \frac{|\mathbf{E}_1|}{|\mathbf{E}_s|}\left\langle \frac{1}{T-t}\int_t^T \lambda[\mathbf{k}(t'-t)] \times A[\mathbf{k}(t')]dt' - \frac{1}{\tau M}\sum_{i=1}^{M} A[\mathbf{k}(t_i+t)]\right\rangle. \tag{1}$$

Here T denotes the total simulation time, τ is the mean free-flight time, M is the number of the scattering events, t_i is the time of the ith scattering event and $\mathbf{k}(t')$ is the wave vector at time t'. For example, if $A = v_{E_1}$ is the velocity component parallel to $\mathbf{E}_1$, then $K_A(t) = \mu_{E_1}(t)$ is the longitudinal differential mobility. Apparently, investigation of the zero-field case $\mathbf{E}_s = 0$ is not possible with Eq. (1).

For a general angle between the small signal and stationary fields the response function can be obtained by a direct simulation of the distribution function gradient over a single-particle trajectory.[4]

Another stationary-field algorithm is based on the simulation of many particle trajectories. The algorithm, which allows independent orientations of the small signal and stationary fields, has been applied to the calculation of the differential mobility tensor.[1] A set of $2N$ particles is followed under the action of a stationary field until the steady state is reached. The set is then divided into equal halves, referred to as P (plus) and M (minus) sets. The components of the wave vectors of set P are shifted by Δk_α along the α axis and those of set M by $-\Delta k_\alpha$. The time is reset and the simulation is continued. The differential mobility function is ob-

tained as the difference between the P and M ensemble averages

$$\mu_{\beta\alpha}(t)=\frac{-q}{2\hbar\Delta k_\alpha}[\langle v_\beta\rangle_P(t)-\langle v_\beta\rangle_M(t)], \tag{2}$$

where v_β is the velocity component along the β axis.

B. Transient field description

In the transient algorithms the stationary field and the small signal field are applied sequentially in time. The carrier system is initially in a steady state. At time zero the small signal field is superimposed, so that the total field becomes time dependent.

The following derivation is based on the transient BE. To retain this equation linear in the distribution function many-body effects such as carrier–carrier scattering and degeneracy effects are neglected. The governing equation for the linear small signal response is obtained by substituting

$$\mathbf{E}(t)=\mathbf{E}_s+\mathbf{E}_1(t)$$

and

$$f(\mathbf{k},t)=f_s(\mathbf{k})+f_1(\mathbf{k},t) \tag{3}$$

into the transient BE and keeping only first order perturbation terms. The small signal field $\mathbf{E}_1(t)$ is some general function of time. To zero order the stationary BE is obtained

$$\frac{q}{\hbar}\mathbf{E}_s\cdot\nabla f_s(\mathbf{k})=Q[f_s(\mathbf{k})]=\int S(\mathbf{k}',\mathbf{k})f_s(\mathbf{k}')d\mathbf{k}-\lambda(\mathbf{k})f_s(\mathbf{k}). \tag{4}$$

Here $S(\mathbf{k}',\mathbf{k})d\mathbf{k}$ denotes the scattering rate from a state with wave vector $\mathbf{k}'$ to states in $d\mathbf{k}$ around $\mathbf{k}$, $\lambda(\mathbf{k})=\int S(\mathbf{k},\mathbf{k}')d\mathbf{k}'$ is the total scattering rate, and q is the charge of a particle. The distribution function f_s is assumed to be normalized to unity, $\int f_s(\mathbf{k})d\mathbf{k}=1$.

The first order equation is linear in the perturbation $\mathbf{E}_1$ and contains the solution of Eq. (4) on the right hand side

$$\frac{\partial f_1(\mathbf{k},t)}{\partial t}+\frac{q}{\hbar}\mathbf{E}_s\cdot\nabla f_1(\mathbf{k},t)=Q[f_1(\mathbf{k},t)]-\frac{q}{\hbar}\mathbf{E}_1(t)\cdot\nabla f_s(\mathbf{k}). \tag{5}$$

Provided that the norm of $f=f_s+f_1$ is conserved (Sec. III), the statistical average can be expressed as

$$\langle A\rangle(t)=\langle A\rangle_s+\langle A\rangle_1(t)=\int A(\mathbf{k})f_s(\mathbf{k})d\mathbf{k}+\int A(\mathbf{k})f_1(\mathbf{k},t)d\mathbf{k}. \tag{6}$$

In the literature the transient BE with an impulse added to a stationary electric field has neither been solved by the common Monte Carlo method, presumably since the latter relies on the physical transparency of the model, nor by deterministic methods. Instead, it is common practice to consider a step-like perturbation $\mathbf{E}_1(t)=\mathbf{E}_{\text{step}}\theta(t)$. The impulse response $\langle A\rangle_{\text{imp}}(t)$ is obtained by taking the time derivative of the step response $\langle A\rangle_{\text{step}}(t)$. To this physically transparent case the ensemble Monte Carlo (EMC) method is applicable. An ensemble of particles is simulated until a steady state is reached under the action of $\mathbf{E}_s$. After that the field is changed abruptly to $\mathbf{E}_s+\mathbf{E}_{\text{step}}$ and the time is reset. The step response function $\langle A\rangle_{\text{step}}(t)$ is given by the time evolution of the ensemble average of A. One drawback of this approach is that the BE solved is not linear with respect to the perturbation $\mathbf{E}_{\text{step}}$. If a small perturbation is assumed, the statistical uncertainty in the results will be very large. The situation is even aggravated by the fact that the derivative of the stochastically obtained step response needs to be taken.[5]

Deterministic methods are not affected by the problem of statistical uncertainty. The method reported in Ref. 6 solves the linearized BE, Eq. (5), for the case of a step-like perturbation.

III. THE PHYSICAL MODEL

The main advantage of the Monte Carlo method is that it allows us to incorporate very complex physical models of semiconductor transport.[7] It is thus desirable to develop Monte Carlo algorithms that can simulate the impulse response directly. For this purpose Eq. (5) is reformulated as an integral equation. A phase space trajectory $\mathbf{K}(t')=\mathbf{k}-(q/\hbar)\mathbf{E}_s(t-t')$ is introduced, which solves the equation of motion given by Newton's law. Initial time and initial value are t and $\mathbf{k}$, respectively, so that $\mathbf{K}(t)=\mathbf{k}$. Since the left hand side of Eq. (5) represents a total time derivative the equation can be formally written as an ordinary first order differential equation $(d/dt)f(t)=-\lambda(t)f(t)+g(t)$. Here the outscattering term λf has been separated from the operator Q. The remainder of the right hand side of Eq. (5) is included in g. The differential equation has the following solution:

$$f(t)=\int_{t_0}^{t}g(t')e^{-\int_{t'}^{t}\lambda(y)dy}dt'+f(t_0)e^{-\int_{t_0}^{t}\lambda(y)dy}, \tag{7}$$

where $f(t_0)$ is the initial condition at time t_0. This result allows us to rewrite Eq. (5) as an integral equation

$$f_1(\mathbf{k},t)=\int_{0-}^{t}dt'\int d\mathbf{k}'f_1(\mathbf{k}',t')S[\mathbf{k}',\mathbf{K}(t')]\times e^{-\int_{t'}^{t}\lambda[\mathbf{K}(y)]dy}-\int_{0-}^{t}\frac{q}{\hbar}\mathbf{E}_1(t')\times(\nabla f_s)[\mathbf{K}(t')]e^{-\int_{t'}^{t}\lambda[\mathbf{K}(y)]dy}dt'. \tag{8}$$

Here we assumed that the small signal field $\mathbf{E}_1(t)$ is zero at negative time, so that the initial condition $f_1[\mathbf{K}(t_0),t_0]=0$ for $t_0<0$. The difference between Eq. (8) and the integral form of the BE (e.g., Refs. 8 and 9) lies in the free term, i.e., the last term on the right hand side of Eq. (8). In the BE the free term F is determined by the initial distribution $f_0(\mathbf{k})\geqslant 0$ of the ensemble

$$F(\mathbf{k})=f_0[\mathbf{K}(0)]e^{-\int_0^t\lambda[\mathbf{K}(y)]dy}. \tag{9}$$

We now consider Eq. (8) for the case of an impulse $\mathbf{E}_1(t)=\delta(t)\mathbf{E}_{\text{im}}$

$$f_{\mathrm{im}}(\mathbf{k},t)=\int_0^t dt'\int d\mathbf{k}' f_{\mathrm{im}}(\mathbf{k}',t')S[\mathbf{k}',\mathbf{K}(t')] \times e^{-\int_{t'}^{t}\lambda[\mathbf{K}(y)]dy}+G(\mathbf{K}(0))e^{-\int_0^t\lambda[\mathbf{K}(y)]dy}, \quad (10)$$

$$G(\mathbf{k})=-\frac{q}{\hbar}\mathbf{E}_{\mathrm{im}}\cdot\nabla f_s(\mathbf{k}). \quad (11)$$

The free term of Eq. (10) is formally equivalent to Eq. (9). The only difference is that G also takes on negative values, and can therefore not be interpreted as an initial distribution. However, without loss of generality G can be expressed as a difference of two positive functions, $G=G^+-G^-$, giving rise to a decomposition of Eq. (10) into two integral equations

$$f^{\pm}_{\mathrm{im}}(\mathbf{k},t)=\int_0^t dt'\int d\mathbf{k}' f^{\pm}_{\mathrm{im}}(\mathbf{k}',t')S[\mathbf{k}',\mathbf{K}(t')] \times e^{-\int_{t'}^{t}\lambda[\mathbf{K}(y)]dy}+G^{\pm}(\mathbf{K}(0))e^{-\int_0^t\lambda[\mathbf{K}(y)]dy}. \quad (12)$$

Equation (12) represents two Boltzmann equations with the initial conditions

$$f^{\pm}_{\mathrm{im}}(\mathbf{k},0)=G^{\pm}(\mathbf{k})\geqslant 0. \quad (13)$$

Equation (10) is obtained by subtracting the two equations. It holds that $f_{\mathrm{im}}(\mathbf{k},t)=f^{+}_{\mathrm{im}}(\mathbf{k},t)-f^{-}_{\mathrm{im}}(\mathbf{k},t)$.

The impulse response distribution function f_{im} has the following property. From Eq. (11) it results that $\int G(\mathbf{k})d\mathbf{k}=0$, such that the norms of the two functions $f^{\pm}_{\mathrm{im}}$ are equal at $t=0$. The BE conserves the normalization during the evolution, provided that no generation or recombination processes are included. Hence $\int f_{\mathrm{im}}(\mathbf{k},t)d\mathbf{k}=0$ for all t. It follows that $\int f(\mathbf{k},t)d\mathbf{k}=\int f_s(\mathbf{k})d\mathbf{k}=1$, which is the prerequisite for Eq. (6) to hold.

The two equations, Eq. (12), are linear in the amplitude $\mathbf{E}_{\mathrm{im}}$, and so is the small signal response $\langle A\rangle_{\mathrm{im}}(t)$. Due to linearity, the response to a field with general time dependence can be obtained from the impulse response by convolution.

In this way we can assign to the impulse response, Eq. (5), the following physical model. The impulse in the electric field at $t=0$ creates instantaneously an initial condition G, corresponding to two carrier ensembles P and M, which are initially distributed according to G^+ and G^-. The two ensembles, which contain the same numbers of particles, evolve in time under the action of the stationary field. The impulse response $\langle A\rangle_{\mathrm{im}}(t)$ is given by the difference of the two ensemble mean values of A

$$\langle A\rangle_{\mathrm{im}}(t)=\langle A\rangle_P(t)-\langle A\rangle_M(t). \quad (14)$$

For long evolution times the two ensembles relax to the same steady state characterized by the distribution f_s,

$$f^{\pm}_{\mathrm{im}}(\mathbf{k},t\to\infty)=Cf_s(\mathbf{k}), \quad (15)$$

where $C=\int G^{\pm}(\mathbf{k})d\mathbf{k}$. Consequently, an impulse response vanishes for large time, $\langle A\rangle_{\mathrm{im}}(t\to\infty)=0$. For practical applications the relaxation process has to be followed for some characteristic time T, which depends on the physical conditions, the semiconductor, and the stationary field. It has a typical values from a few ps to a few hundreds of ps, as shown in Sec. V.

IV. THE MONTE CARLO METHOD

Due to the freedom in treating the term G and in choosing a decomposition $G=G^+-G^-$ one can devise a variety of Monte Carlo algorithms. Once the initial conditions $G^{\pm}$ are provided, the relaxation process of the two subensembles can be simulated with the common EMC method.

A. The finite difference approximation

An obvious possibility is to approximate ∇f_s by a finite difference quotient. The central difference quotient gives

$$G(\mathbf{k})\simeq-\frac{q}{\hbar}|\mathbf{E}_{\mathrm{im}}|\left(\frac{f_s(\mathbf{k}+\Delta\mathbf{k}_1)-f_s(\mathbf{k}-\Delta\mathbf{k}_1)}{2|\Delta\mathbf{k}_1|}\right). \quad (16)$$

The vectors $\Delta\mathbf{k}_1$ and $\mathbf{E}_{\mathrm{im}}$ have to be collinear, while $\mathbf{E}_{\mathrm{im}}$ and $\mathbf{E}_s$ may have arbitrary directions. The two terms provide the initial distribution functions $G^{\pm}$ of the P and M ensembles. The drawback of the method is that the solution depends on $\Delta\mathbf{k}_1$. Choosing a small magnitude to stay in the linear region will result in very similar distributions $G^{\pm}$ and hence in a large statistical uncertainty in the result due the subtraction of nearly equal averages.

1. Algorithm 1

The first task of the simulation is to provide a set of N $\mathbf{k}$ values with the distribution $f_s(\mathbf{k})$. The EMC method can be used to evolve an ensemble of N particles until a steady state is reached. Then a displacement of the states $\mathbf{k}$ by $\Delta\mathbf{k}_1$ (by $-\Delta\mathbf{k}_1$) gives the initial points for the trajectories of the P (the M) ensembles at $t=0$. The impulse response function of a quantity A is given by Eq. (14), multiplied by $-q|\mathbf{E}_{\mathrm{im}}|/(2\hbar|\Delta\mathbf{k}_1|)$. This algorithm corresponds essentially to the one proposed by Price[1] (see Sec. II) with the extension that arbitrary quantities A are treated.

2. Algorithm 2

If a trajectory $\mathbf{K}(t)$ evolving in a stationary field is sampled at discrete times $t_j=j\Delta t$, the values $\mathbf{k}_j=\mathbf{K}(t_j)$ will be distributed with f_s. This result follows from the equivalence of the ensemble and time averages in the steady state. In this way a single-particle Monte Carlo algorithm can be used to generate the initial states for an EMC algorithm. At time t_j the evolution of the single-particle trajectory is interrupted. The current state $\mathbf{k}$ is then used to determine the starting point of one P trajectory as $\mathbf{k}+\Delta\mathbf{k}_1$ and that of one M trajectory at $\mathbf{k}-\Delta\mathbf{k}_1$. The P and M trajectories are then followed for a time T, and the contribution to the response function is recorded. After that the single particle trajectory is continued for another Δt, and the procedure is repeated. The main steps are:

(1) Follow a main trajectory for Δt and determine the state $\mathbf{k}$ in the endpoint.
(2) Start a trajectory $\mathbf{K}^+(t)$ from $\mathbf{k}+\Delta\mathbf{k}_1$ and another trajectory $\mathbf{K}^-(t)$ from $\mathbf{k}-\Delta\mathbf{k}_1$.

(3) Follow both trajectories for time T. At equidistant times t_i add $A[\mathbf{K}^+(t_i)]$ to a histogram ν_i^+ and $A[\mathbf{K}^-(t_i)]$ to a histogram ν_i^-.
(4) Continue with the first step until N $\mathbf{k}$ points have been generated.
(5) Calculate the time discrete impulse response as $\langle A\rangle_{\mathrm{im}}(t_i)=(-qE_{\mathrm{im}}/2N\hbar\Delta k_1)(\nu_i^+-\nu_i^-)$.

B. The longitudinal perturbation

In the case that the stationary and the small signal field vectors are collinear, the stationary BE, Eq. (4), can be used to express the distribution function gradient as

$$G(\mathbf{k})=\frac{E_{\mathrm{im}}}{E_s}\left(\lambda(\mathbf{k})f_s(\mathbf{k})-\int f_s(\mathbf{k}')S(\mathbf{k}',\mathbf{k})d\mathbf{k}'\right), \quad (17)$$

which gives another natural splitting into two positive functions. In the following we adopt the notation that terms which are employed in the respective algorithm as a probability density are enclosed in curly brackets.

1. Algorithm 3

From Eq. (17) we choose the initial distributions as

$$G^+(\mathbf{k})=\frac{E_{\mathrm{im}}}{E_s}\lambda(\mathbf{k})\{f_s(\mathbf{k})\}, \quad (18)$$

$$G^-(\mathbf{k}')=\frac{E_{\mathrm{im}}}{E_s}\int\{f_s(\mathbf{k})\}\left\{\frac{S(\mathbf{k},\mathbf{k}')}{\lambda(\mathbf{k})}\right\}\lambda(\mathbf{k})d\mathbf{k}. \quad (19)$$

Both terms contain f_s as a probability density. States $\mathbf{k}$ can be generated from this density as in Algorithm 2. In addition, in G^- the density $\lambda^{-1}S$ appears, which is the conditional probability density for an after-scattering state $\mathbf{k}'$ provided that the initial state $\mathbf{k}$ has been selected. Note that normalization is ensured, since $\int\lambda(\mathbf{k})^{-1}S(\mathbf{k},\mathbf{k}')d\mathbf{k}'=1$ for all $\mathbf{k}$.

The above expressions suggest the following algorithm:

(1) Follow a main trajectory for Δt. Determine the state $\mathbf{k}$ in the endpoint and the weight $\lambda(\mathbf{k})$.
(2) Realize a scattering event from $\mathbf{k}$ to $\mathbf{k}'$.
(3) Start a trajectory $\mathbf{K}^+(t)$ from $\mathbf{k}$ and another trajectory $\mathbf{K}^-(t)$ from $\mathbf{k}'$.
(4) Follow both trajectories for time T. At equidistant times t_i add $\lambda(\mathbf{k})A[\mathbf{K}^+(t_i)]$ to a histogram ν_i^+ and $\lambda(\mathbf{k})A[\mathbf{K}^-(t_i)]$ to a histogram ν_i^-.
(5) Continue with the first step until N $\mathbf{k}$ points have been generated.
(6) Calculate the time discrete impulse response as $\langle A\rangle_{\mathrm{im}}(t_i)=(E_{\mathrm{im}}/NE_s)(\nu_i^+-\nu_i^-)$.

2. Algorithm 4

We reformulate the initial distributions as follows:

$$G^+(\mathbf{k})=\frac{E_{\mathrm{im}}}{E_s}\langle\lambda\rangle_s\left\{\frac{\lambda(\mathbf{k})f_s(\mathbf{k})}{\langle\lambda\rangle_s}\right\}, \quad (20)$$

$$G^-(\mathbf{k}')=\frac{E_{\mathrm{im}}}{E_s}\langle\lambda\rangle_s\int\left\{\frac{\lambda(\mathbf{k})f_s(\mathbf{k})}{\langle\lambda\rangle_s}\right\}\left\{\frac{S(\mathbf{k},\mathbf{k}')}{\lambda(\mathbf{k})}\right\}d\mathbf{k}, \quad (21)$$

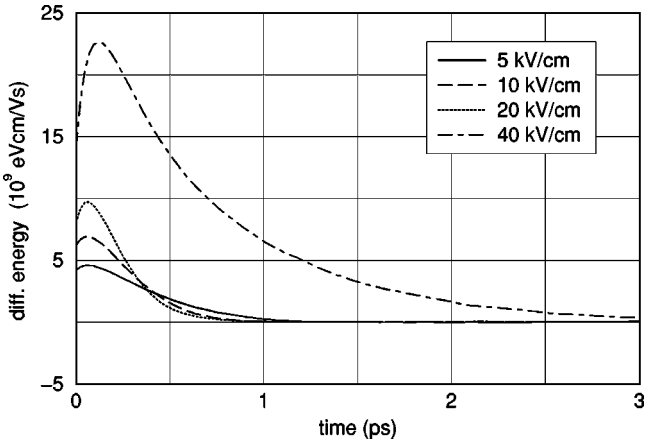

FIG. 1. Impulse response of the differential energy.

where $\langle\lambda\rangle_s=\int f_s(\mathbf{k})\lambda(\mathbf{k})d\mathbf{k}$ is introduced in the denominators to ensure normalization. $\langle\lambda\rangle_s$ is the inverse of the mean free-flight time, which can be seen immediately when evaluating the average by means of the before-scattering method. The probability density $\lambda f_s/\langle\lambda\rangle_s$ represents the normalized distribution function of the before-scattering states. Consequently, the product of the two densities in Eq. (21) represents the normalized distribution function of the after-scattering states. Compared with Algorithm 3 a more compact algorithm can be formulated.

(1) Follow a main trajectory for one free flight, store the before-scattering state in $\mathbf{k}_b$, and realize a scattering event from $\mathbf{k}_b$ to $\mathbf{k}_a$.
(2) Start a trajectory $\mathbf{K}^+(t)$ from $\mathbf{k}_b$ and another trajectory $\mathbf{K}^-(t)$ from $\mathbf{k}_a$.
(3) Follow both trajectories for time T. At equidistant times t_i add $A[\mathbf{K}^+(t_i)]$ to a histogram ν_i^+ and $A[\mathbf{K}^-(t_i)]$ to a histogram ν_i^-.
(4) Continue with the first step until N $\mathbf{k}$ points have been generated.
(5) Calculate the time discrete impulse response as $\langle A\rangle_{\mathrm{im}}(t_i)=(E_{\mathrm{im}}\langle\lambda\rangle_s/NE_s)(\nu_i^+-\nu_i^-)$.

The mean free-flight time must be additionally calculated during the simulation. Algorithm 4 shows in a transparent

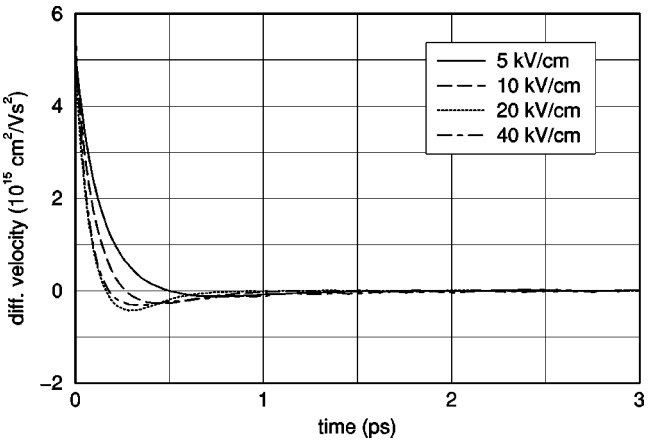

FIG. 2. Impulse response of the differential velocity.

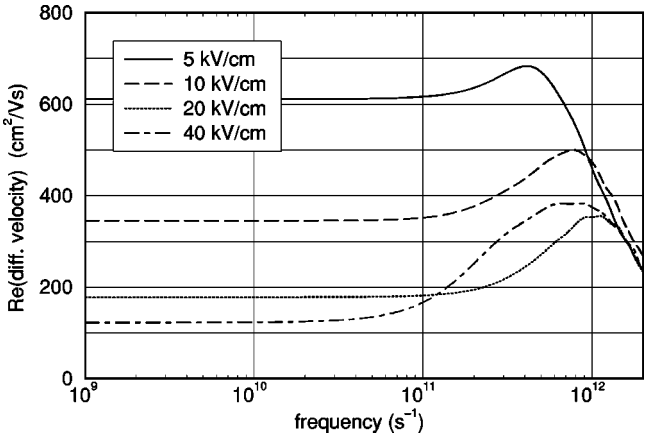

FIG. 3. Real part of the differential velocity spectra.

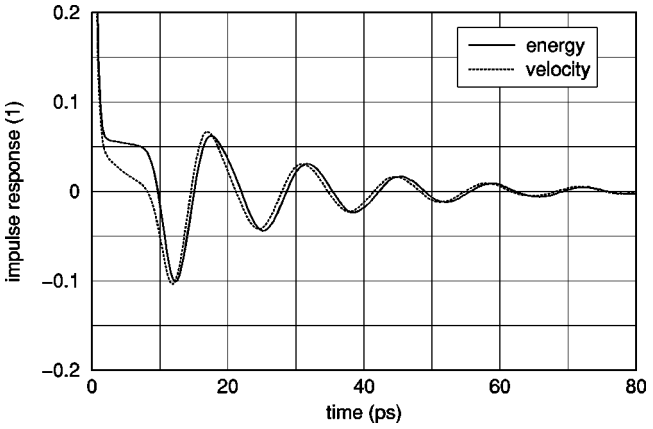

FIG. 5. Impulse response of the normalized differential energy and velocity.

way the evolution of the P and M ensembles, as well as the generation of the initial states for those ensembles.

The algorithm suggested in Ref. 3, leading to Eq. (1), appears to be a single particle equivalent to the described algorithms. A trajectory $\mathbf{K}^-$, which starts from an after-scattering state in Algorithm 4, can immediately be mapped onto the main trajectory and need not be calculated independently. This change gives the second term on the right hand side of Eq. (1). The time integral in Eq. (1) represents a time average that is equivalent to the P ensemble average used in Algorithm 3. The present derivation shows that in practical simulations the averaging interval $(T-t)$ in Eq. (1) should be replaced by a constant value T', which is large enough to capture the whole relaxation process. If T' is larger than a few times the related relaxation time there will no more information to be gained and the statistical uncertainty of the result will even increase.

V. RESULTS

The following simulation results are obtained by using Algorithm 4. Typical conditions for electrons in Si are considered as well as a special carrier dynamics feature, the transit time resonance (TTR) effect[4,10] for electrons in GaAs. While Si is simulated at 300 K, for GaAs the temperature is reduced to 10 K to make the TTR effect clearly visible.

Analytical band models are adopted for both Si and GaAs, accounting for isotropic and nonparabolic conduction band valleys. For Si six equivalent X valleys and for GaAs a three-valley model are included. The phonon scattering rates used can be found, for example, in Ref. 7. Overlap integrals are neglected, and acoustic deformation potential scattering is assumed elastic.

Figures 1 and 2 show the time response of the differential electron energy $\partial\langle\epsilon\rangle_{\mathrm{im}}/\partial E_{\mathrm{im}}$ and the longitudinal differential velocity $\partial\langle v\rangle_{\mathrm{im}}/\partial E_{\mathrm{im}}$ for Si at different field strengths. As expected from the discussion of the model [see Eq. (14)], the response characteristics tend to zero when the two ensembles approach the steady state. The characteristic time associated with the relaxation process depicted in Fig. 2, namely the momentum relaxation time, clearly decreases with increasing field. This effect is anticipated since the electron mobility $\mu = e\tau_m/m^*$ is known to show such a field reduction. Generally, within a few picoseconds the steady state is reached by the two ensembles.

Figures 3 and 4 show the frequency dependence of the differential velocity obtained by a Fourier transform of the impulse response. The low frequency limits of the imaginary parts tend to zero, while the real parts tend to the corresponding differential mobility values $\partial\langle v\rangle_s/\partial E_s$.

For electrons in GaAs the assumed physical conditions are $T = 10$ K and $E_s = 120$ V/cm. In this case all electrons are

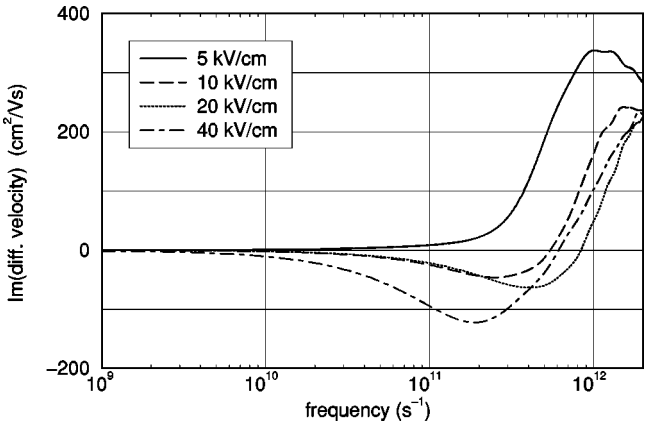

FIG. 4. Imaginary part of the differential velocity spectra.

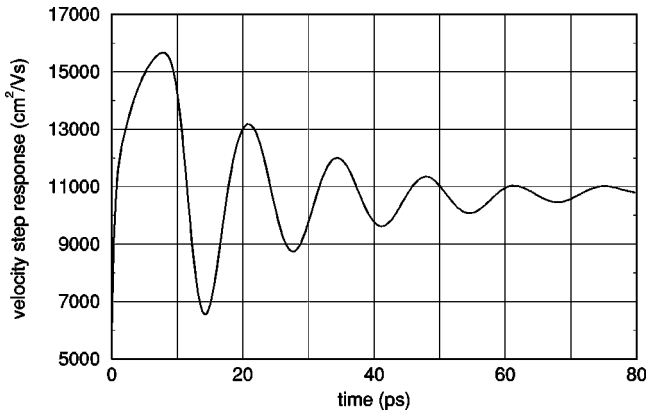

FIG. 6. Step response of the differential velocity.

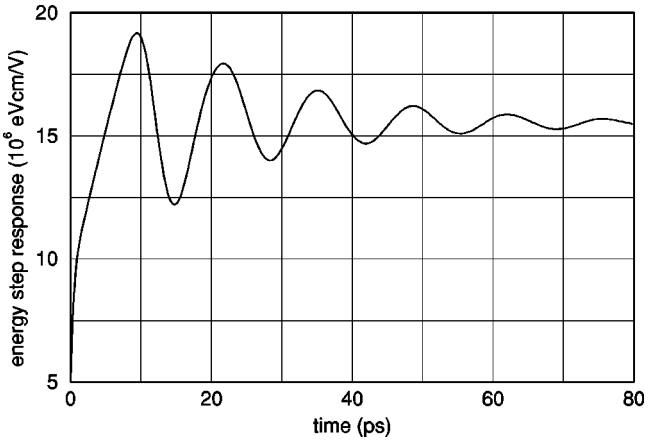

FIG. 7. Step response of the differential energy.

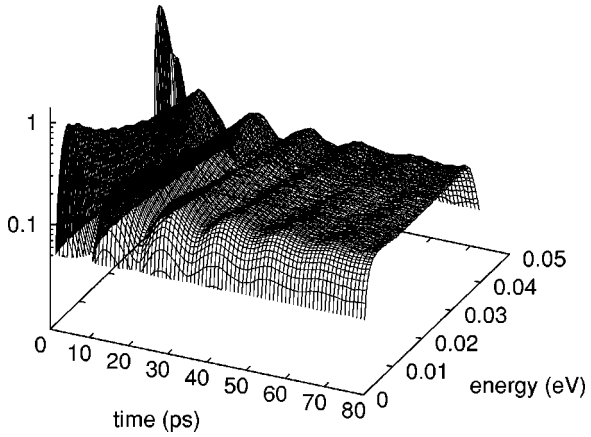

FIG. 9. Evolution of the distribution function of the P ensemble.

in the Γ valley. In Fig. 5 the differential velocity and differential energy are presented normalized to the respective initial values. The impulse response characteristics reveal a damped oscillation. The pattern is pronounced also in the step response functions in Figs. 6 and 7, obtained by time integration of the corresponding impulse response functions. The pattern appears to be independent of the concrete physical quantity, which leads to the conclusion that a peculiarity of the carrier dynamics is responsible for the behavior. The chosen physical conditions determine a peculiar behavior of the electrons already in the steady state. Since acoustic phonon scattering is low (below one scattering for 100 ps), the electrons are accelerated by the field until they reach energies above the polar-optical phonon energy (0.036 eV). Above this energy the scattering rate for phonon emission increases rapidly, so that the electrons penetrating the phonon threshold are intensively scattered back to energies close to zero.

The effect can most conveniently be discussed in the energy domain. The field impulse instantaneously creates a perturbation, represented by ensembles P and M with initial distributions G^+ and G^-, respectively. Figure 8 shows the distributions as two peaks, located close to $E=0$ and above the phonon threshold. The M ensemble is accelerated by the field toward the phonon threshold. The P ensemble is intensively transferred within less than 2 ps back to low energies and is then accelerated by the electric field.

Figures 9 and 10 show the individual evolution of the two ensembles. The initial peaks broaden toward the steady state, which is reached at about 80 ps.

The M ensemble undergoes an evolution similar to that of the P ensemble, however with some delay. This is demonstrated in Fig. 8 where the two distribution functions are shown at $t=8$ ps. The time delay in the evolution is responsible for the oscillation in $\langle A\rangle_{\mathrm{im}}(t)$. If the two distributions were equivalent at a certain time, they would oscillate synchronously for later times and no oscillation in $\langle A\rangle_{\mathrm{im}}(t)$ would show up

For the condition considered each electron undergoes a permanent cycle in the energy domain. The TTR effect occurs since the two ensembles collectively follow this single particle behavior during a certain transition time.

VI. CONCLUSION

A linearized form of the transient BE is used to investigate the small signal response of carriers in semiconductors. Assuming an impulse-like perturbation in the electric field

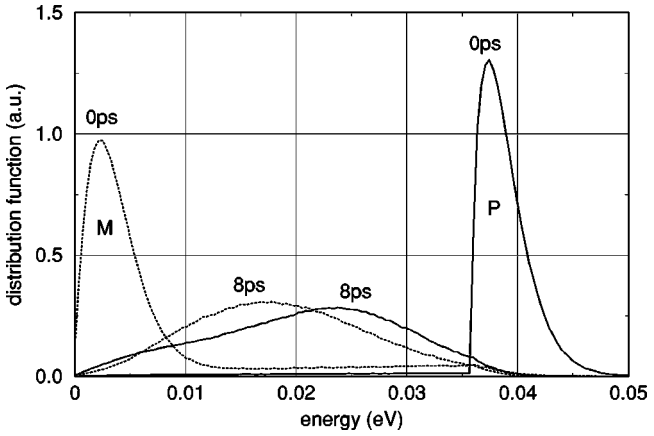

FIG. 8. Energy distribution of the P and M ensembles at $t=0$ and $t=8$ ps.

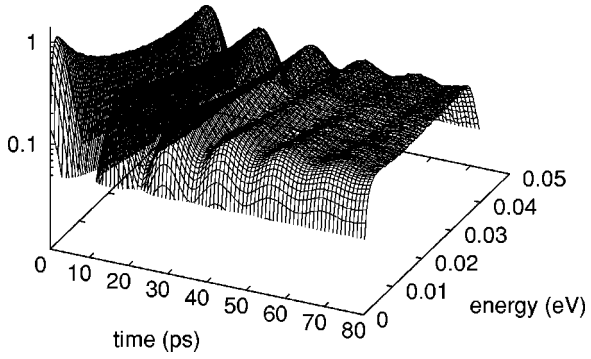

FIG. 10. Evolution of the distribution function of the M ensemble.

the linearized equation is split into two common BEs, which are solved by the EMC method. In this way the impulse response is understood in terms of the concurrent time evolution of two carrier ensembles. Using different methods to provide the initial distributions of the two ensembles leads to a variety of Monte Carlo algorithms. Both existing and new Monte Carlo algorithms are obtained in a unified way, and a transparent, physical interpretation of the algorithms is provided.

ACKNOWLEDGMENT

This work was partially supported by the FWF, Austria, Project No. P13333-TEC.

[1] P. Price, J. Appl. Phys. **54**, 3616 (1983).
[2] L. Reggiani, E. Starikov, P. Shiktorov, V. Gružinskis, and L. Varani, Semicond. Sci. Technol. **12**, 141 (1997).
[3] V. Gružinskis, E. Starikov, and P. Shiktorov, Solid-State Electron. **36**, 1055 (1993).
[4] E. Starikov and P. Shiktorov, Sov. Phys. Semicond. **22**, 45 (1988).
[5] E. Starikov, P. Shiktorov, V. Gruzinskis, L. Varrani, J. Vaissiere, J. Nougier, and L. Reggiani, J. Appl. Phys. **79**, 242 (1996).
[6] J. Vaissiere, J. Nougier, L. Varrani, P. Houlet, L. Hlou, E. Starikov, P. Shiktorov, and L. Reggiani, Phys. Rev. B **49**, 11144 (1994).
[7] C. Jacoboni and P. Lugli, *The Monte Carlo Method for Semiconductor Device Simulation* (Springer, Wien, 1989).
[8] M. Nedjalkov and P. Vitanov, Solid-State Electron. **33**, 407 (1990).
[9] L. Rota, C. Jacoboni, and P. Poli, Solid-State Electron. **32**, 1417 (1989).
[10] Y. Pozhela, E. Starikov, and P. Shiktorov, Semicond. Sci. Technol. **7**, B386 (1992).